NIH Public Access
Author Manuscript

Motesanib (AMG706), a potent multikinase inhibitor, antagonizes multidrug resistance by inhibiting the efflux activity of the ABCB1

Yi-Jun Wang[a], **Rishil J. Kathawala**[a], **Yun-Kai Zhang**[a], **Atish Patel**[a], **Priyank Kumar**[a], **Suneet Shukla**[b], **King Leung Fung**[b], **Suresh V. Ambudkar**[b], **Tanaji T. Talele**[a], and **Zhe-Sheng Chen**[a,*]

[a]Department of Pharmaceutical Sciences, College of Pharmacy and Health Sciences, St. John's University, Queens, NY 11439, USA

[b]Laboratory of Cell Biology, Center for Cancer Research, National Cancer Institute, NIH, Bethesda, MD 20892, USA

Abstract

Cancer cells often become resistant to chemotherapy through a phenomenon known as multidrug resistance (MDR). Several factors are responsible for the development of MDR, preeminent among them being the accelerated drug efflux mediated by overexpression of ATP binding cassette (ABC) transporters. Some small molecule tyrosine kinase inhibitors (TKIs) were recently reported to modulate the activity of ABC transporters. Therefore, the purpose of this study was to determine if motesanib, a multikinase inhibitor, could reverse ABCB1-mediated MDR. The results showed that motesanib significantly sensitized both ABCB1-transfected and drug-selected cell lines overexpressing this transporter to its substrate anticancer drugs. Motesanib significantly increased the accumulation of [^{3}H]-paclitaxel in ABCB1 overexpressing cells by blocking the efflux function of ABCB1 transporter. In contrast, no significant change in the expression levels and localization pattern of ABCB1 was observed when ABCB1 overexpressing cells were exposed to 3 μM motesanib for 72 h. Moreover, motesanib stimulated the ATPase activity of ABCB1 in a concentration-dependent manner, indicating a direct interaction with the transporter. Consistent with these findings, the docking studies indicated favorable binding of motesanib within the transmembrane region of homology modeled human ABCB1. Here, we report for the first time, motesanib, at clinically achievable plasma concentrations, antagonizes MDR by inhibiting the efflux activity of the ABCB1 transporter. These findings may be useful for cancer combination therapy with TKIs in the clinic.

*Corresponding Author: Zhe-Sheng Chen, Department of Pharmaceutical Sciences, St. John's University, Queens, New York, 11439. chenz@stjohns.edu, Phone: 1-718-990-1432, Fax: 1-718-990-1877.

Conflicts of Interest: There are no conflicts of interest.

Keywords

Multidrug resistance; ABC transporters; ABCB1; Tyrosine kinase inhibitor; Motesanib

1. Introduction

Cancer, known medically as malignant neoplasm or tumor, is the second most leading cause of death after cardiovascular disease in the United States and developing countries [1]. Cancer treatment is often consisted of surgery, radiation therapy, chemotherapy and combination therapy. Chemotherapy has been the first-line approach for the treatment of most cancers for several decades, and it typically involves systemic administration of combination of anticancer drugs from different chemical groups with different mechanism of action and depends on the capability of highly cytotoxic drugs to penetrate and selectively kill cancer cells [2]. However, cancer cells often exhibit either intrinsic or acquired resistance to chemotherapy through a phenomenon known as multidrug resistance (MDR) [3]. Many factors are responsible for the development of MDR, preeminent among them being the accelerated drug efflux mediated by overexpression of ATP binding cassette (ABC) transporters [4]. These ABC transporters serve as a defense mechanism by pumping harmful substrates out of normal cells. In a similar manner, cancer cells tend to overexpress these transporters in order to protect themselves from cytotoxic anticancer drugs. These transporters efflux drugs by consuming the energy produced via hydrolysis of ATP [5]. So far, 48 human ABC transporters have been identified and categorized into seven subfamilies, from ABCA to ABCG, based on structural and sequence similarities [6]. Among them, ABCB1, ABCG2, and ABCCs are the primary contributors of MDR in cancer cells [7].

ABCB1, also called P-glycoprotein coded by MDR1 gene, was the first discovered mammalian ABC transporter [8,9]. It is comprised of two homologous halves, each containing six transmembrane helices and an ATP binding/utilization domain, separated by a flexible linker. ABCB1 is a 170-kDa apical plasma membrane protein ubiquitously expressed in kidney, placenta, liver, adrenal glands, intestine and blood-brain barrier cells, where it functions to protect against xenobiotics and cellular toxicants [10,11]. In addition, ABCB1 can transport a wide range of anticancer drugs such as doxorubicin, vincristine, paclitaxel, and epipodophyllotoxins out of the cancer cells [7,12]. The overexpression of ABCB1 can be induced after repeated exposure to anticancer drugs, when the tumor becomes refractory to chemotherapy. ABCG2, a 72-kDa protein, is the first known half transporter with only one nucleotide binding domain and one transmembrane domain to mediate MDR [13]. The functional unit of ABCG2 is a homodimer or an oligomer [14]. The wide spectrum of chemotherapeutic agents transported by ABCG2 ranges from organic anion conjugates, nucleoside analogues, organic dyes, tyrosine kinase inhibitors (TKIs) to anthracyclines (such as doxorubicin, mitoxantrone), camptothecin-derived indolocarbazole topoisomerase I inhibitors, methotrexate, and flavopiridols [14]. ABCC1 (MRP1), which is a member of the C subfamily of ABC transporters can also transport various hydrophobic drugs; some anionic drugs and its drug conjugates, including antifolates, certain nucleotides, and also vinca alkaloids [15,16]. ABCC10, also known as multidrug resistance protein 7

(MRP7), is a 171-kDa protein that can transport various anticancer drugs, including docetaxel, paclitaxel, vincristine, vinblastine, cytarabine, gemcitabine and epothilone B [17,18].

In the last three decades, MDR research has mainly focused on developing inhibitors of ABC transporters, which have minimal toxicity in normal cells. It has been reported that some epidermal growth factor receptor (EGFR) TKI inhibitors including AG1478, erlotinib and lapatinib significantly reversed ABCB1- and ABCG2-mediated MDR, indicating that these TKIs might be modulators of ABCB1 and ABCG2 transporters [19]. In addition, BCR-Abl TKIs (imatinib and nilotinib) were also found to reverse ABCB1-and ABCG2-mediated MDR [20]. An *in vivo* study using the combination of gefitinib and a camptothecin derivative has shown a better pharmacokinetic profile and anti-tumor activity compared to camptothecin derivatives alone [21]. Our lab has also reported that the anti-tumor response to paclitaxel was enhanced by lapatinib in ABCB1 overexpressing nude mice tumor xenografts [22]. Moreover, erlotinib, lapatinib, imatinib, and nilotinib significantly reverse ABCC10-mediated MDR [23,24]. Canertinib (CI-1033), a human epidermal receptor (HER) TKI, was found to reverse ABCG2-mediated MDR in cancer cells [25]. Some multikinase TKIs (such as sunitinib) have shown a reversal activity in both ABCB1- and ABCG2-mediated MDR [26,27]. All these *in vitro* and *in vivo* studies reveal that the combination therapy of TKIs and conventional chemotherapeutic drugs could significantly sensitize MDR cells that overexpress diverse ABC transporters. Therefore, given the studies showing that TKIs play a significant role in reversing MDR in cancer cells, it is important to understand their mechanism of action.

Motesanib (AMG706), a novel nicotinamide derivative, was identified as a potent, orally bioavailable inhibitor of the vascular endothelial growth factor receptor 1 (VEGFR1/Flt1), VEGFR2/kinase domain receptor/Flk-1, VEGFR3/Flt4, platelet-derived growth factor receptor (PDGFR) and Kit receptors in preclinical models (Fig. 1A) [28]. In preclinical studies, motesanib induced significant tumor regression in xenograft models of human breast carcinoma [29], non-small cell lung cancer, medullary thyroid cancer, and epidermoid and colon carcinoma [30]. Motesanib is currently under Phase II and Phase III clinical trials for advanced gastrointestinal stromal tumor (GIST), fallopian tube cancer, ovarian cancer, thyroid cancer, non-small cell lung cancer (NSCLC) (www.clinicaltrials.gov). For instance, in the study of patients with imatinib-resistant GIST, motesanib treatment has shown acceptable tolerability and modest tumor control as evident in the proportion of patients who achieved stable disease and durable stable disease [31]. In addition, motesanib can induce partial responses in patients with advanced or metastatic differentiated thyroid cancer that is progressive. However, a broader applicability of motesanib treatment that inhibits angiogenesis in thyroid cancer needs to be established in further studies [32]. The most common side effects of motesanib treatment were diarrhea, fatigue, hypothyroidism, hypertension and anorexia [33]. The analysis of the phase III MONET1 study demonstrated that motesanib combined with carboplatin/paclitaxel could improve overall survival (OS), progression-free survival (PFS) and objective response rate (ORR) compared with chemotherapy alone, in a subset of Asian patients with nonsquamous NSCLC [34]. Importantly, the overexpression of ABCB1 has been associated with various cancers, such

as GIST, NSCLC, fallopian tube, ovarian and thyroid cancer [35–39]. It is conceivable that motesanib probably could inhibit the function of ABC transporters by binding to their drug-binding sites as has been found for other TKIs [19]. This has triggered our efforts to determine if motesanib could reverse MDR, which is associated with the overexpression of ABCB1, ABCG2, ABCC1 and ABCC10.

2. Materials and methods

2.1. Chemicals and equipment

[^{3}H]-paclitaxel (23 Ci/mmol) was purchased from Moravek Biochemicals, Inc (Brea, CA). Dulbecco's modified Eagle's medium (DMEM), RPMI-1640 medium, fetal bovine serum (FBS), penicillin/streptomycin and trypsin 0.25% were products of Hyclone, Thermo Scientific (Logan, UT). The monoclonal antibodies BXP-21 (against ABCG2), sc-47778 (against β-Actin) and the secondary horseradish peroxidase-labeled rabbit anti-mouse IgG were purchased from Santa Cruz Biotechnology, Inc. (Dallas, TX). The monoclonal antibody C219 (against ABCB1) and skim milk powder were purchased from EMD Millipore Corporation (Billerica, MA). The monoclonal antibody P7965 (against ABCB1) was purchased from Sigma Chemical Co. (St. Louis, MO). The Alexa flour 488-conjugated goat anti-mouse IgG was purchased from Molecular Probes (Eugene, OR). Full-Range Rainbow Molecular Weight Marker was purchased from GE healthcare Life Sciences (Pittsburgh, PA). Fumitremorgin C (FTC) was synthesized by Thomas McCloud, Developmental Therapeutics Program, and Natural Products Extraction Laboratory, NIH (Bethesda, MD) and was a gift from Dr. Susan Bates. PAK-104P was a gift of Prof. Shin-Ichi Akiyama (Kagoshima University, Kagoshima, Japan) from Nissan Chemical Ind. Co., Ltd. (Chiba, Japan). Cepharanthine was generously gifted by Kakenshoyaku Co. (Tokyo, Japan). Motesanib (AMG-706) was purchased from ChemieTek (Indianapolis, IN). Mitoxantrone, colchicine, paclitaxel, vincristine, cisplatin, verapamil, Triton X-100, paraformaldehyde, 3-(4,5-dimethylthiazol-yl)-2,5-diphenyl-tetrazolium bromide (MTT), dimethyl sulfoxide (DMSO), ammonium molybdate, MES hydrate, antimony potassium tartrate, sodium azide and N-methyl-D-glucamine were obtained from Sigma Chemical Co. (St. Louis, MO). Potassium phosphate, EGTA and ATP were products of AMRESCO (Solon, OH). Sulfuric acid solution (37N) was purchased from Fisher Scientific (Pittsburgh, PA). KCl was product of Avantor Performance Materials (Center Valley, PA). Ouabain was purchased from Enzo Life Sciences, Inc. (Farmingdale, NY). Dithiothreitol was product of Promega Corporation (Madison, WI). MgCl$_2$ was purchased from EMD Millipore (Billerica, MA). Ascorbic acid was product of VWR International (West Chester, PA). Sodium orthovanadate was purchased from Alfa Aesar (Ward Hill, MA). OPSYS microplate reader was purchased from Dynex Technologies (Chantilly, VA).

2.2. Cell lines and cell culture

The KB-C2 cell line overexpressing ABCB1, was established by a step-wise exposure of KB-3-1, the parental human epidermoid carcinoma cell line, to increasing concentration of colchicine up to 2 μg/ml [40]. The LLC-PK1 porcine kidney epithelial cell line and LLC-MDR1-WT transfected with human ABCB1 cDNA were as previously described [41]. HEK293/pcDNA3.1, HEK/ABCC1 and HEK/ABCC10 cells were generated by transfecting

the HEK293 cells with empty vector, ABCC1 expression vector and ABCC10 expression vector, respectively [42]. HEK/ABCC1 was generated in Dr. Ambudkar's laboratory (NCI, NIH, Bethesda, MD) and the plasmid containing ABCC10 was generously provided by the late Dr. Gary Kruh (University of Illinois at Chicago, Chicago, IL). Transfected cells were selected in DMEM containing 2 mg/ml G418. The parental human non-small cell lung cancer cell line NCI-H460 was grown in RPMI-1640 medium supplemented with 10% heat-inactivated fetal bovine serum. The resistant NCI-H460/MX20 cell line overexpressing ABCG2, was cultured in the above-mentioned medium with addition of 20 nM mitoxantrone. Both NCI-H460 and NCI-H460/MX20 cells were kindly provided by Drs. Susan Bates and Robert Robey (NCI, NIH, Bethesda, MD). All other cell lines were cultured at 37°C, 5% CO_2 with DMEM containing 10% FBS and 1% penicillin/streptomycin. All cells were grown as adherent monolayer in drug-free culture media for more than 2 weeks before assay.

2.3. Cytotoxicity determination by MTT assay

The modified MTT colorimetric assay was used to detect the sensitivity of cells to anticancer drugs *in vitro* [44]. Briefly, cells were seeded in 180 μl medium in 96-well plates in triplicate at 5000~6000 cells/well. After the incubation at 37°C for 24 h, cells were pre-incubated with or without the reversal agents (20 μl/well) for 2 h and then different concentrations of chemotherapeutic drugs (20 μl/well) were added into designated wells. After 72 h of incubation at 37 °C, 20 μl of MTT solution (4 mg/ml) was added to each well. The plates were further incubated at 37°C for 4 h, allowing viable cells to change the yellow-colored MTT into dark-blue formazan crystals. Subsequently, the MTT/medium was removed from each well without disturbing the cells, and 100 μl of DMSO was added into each well. Plates were placed on a shaking table to thoroughly mix the formazan into the solvent. Finally, the absorbance was determined at 570 nm by Opsys microplate reader (Dynex Technologies, Chantilly, VA). The degree of resistance was calculated by dividing the IC50 for the MDR cells with or without inhibitors by that of the parental cells without inhibitor. The concentrations of motesanib as a potential reversal agents used in this study were 1 μM and 3 μM. Verapamil, FTC and cepharanthine were used at nontoxic concentration of 3 μM as positive controls for inhibiting ABCB1, ABCG2 and ABCC10, respectively.

2.4. [3H]-Paclitaxel accumulation assay

The accumulation of [3H]-paclitaxel in KB-3-1 and KB-C2 cells was measured in the absence or presence of motesanib at 1 μM and 3 μM, and verapamil at 3 μM [45]. Cells were trypsinized and four aliquots from each cell line were resuspended in the DMEM medium in four centrifuge tubes. The suspended cells were preincubated with or without reversal drugs for 2 h at 37°C in DMEM medium. To measure drug accumulation, cells were subsequently incubated with 0.01 μM [3H]-paclitaxel for 2 h in the presence or absence of the reversal drugs at 37°C. After washing three times with ice cold PBS, the cells were pelleted and placed in lysis buffer (pH 7.4, containing 1% Triton X-100 and 0.2% SDS). Each sample was placed in a scintillation vial with 5 ml scintillation fluid and radioactivity was measured in a Packard TRI-CARB 1900CA liquid scintillation analyzer from Packard Instrument Company, Inc (Downers Grove, IL).

2.5. [^{3}H]-Paclitaxel efflux assay

In the efflux study cells were also incubated with 0.01 μM [^{3}H]-paclitaxel according to the method used in the accumulation study [45]. However, after washing three times with ice cold PBS, the suspended cells were incubated at 37°C in fresh DMEM medium with or without reversal drugs. After 0, 30, 60, and 120 min, the aliquots of cells were removed and immediately washed three times with ice-cold PBS. The resulting cells were pelleted and placed in lysis buffer (pH 7.4, containing 1% Triton X-100 and 0.2% SDS). Each sample was placed in a scintillation vial with 5 ml scintillation fluid and radioactivity was measured in a Packard TRI-CARB 1900CA liquid scintillation analyzer from Packard Instrument Company, Inc (Downers Grove, IL).

2.6. Preparation of total cell lysates

The cells were treated with or without reversal drugs for different time periods (0 h, 24 h, 48 h, 72 h), then were harvested and rinsed with ice cold PBS for three times. The cell extracts were prepared by incubating cells with lysis buffer (10 mM Tris HCl, pH 7.5, 1 mM EDTA, 0.1% SDS, 150 mM NaCl, 1% Triton X-100 and 0.01% leupeptin) for 30min on ice with occasional rocking, followed by centrifugation at 12,000 rpm at 4°C for 20 min. The supernatant containing total cell lysates was collected and stored at −80°C until the gel electrophoresis was run. Protein concentrations were determined by bicinchoninic acid (BCA™)-based protein assay (Thermo Scientific, Rockford, IL).

2.7. Western blot analysis

Equal amounts of total cell lysates (60 μg protein) and Full-Range Rainbow Molecular Weight Marker were resolved using 8%–12% sodium dodecyl sulfate polyacrylamide gel electrophoresis (SDS-PAGE) and transferred onto polyvinylidene fluoride (PVDF) membranes through electrophoresis. The PVDF membranes were immersed in blocking solution (5% skim milk) in TBST buffer (10 mM Tris–HCl, pH 8.0, 150 mM NaCl, and 0.1% Tween 20) to block nonspecific binding for 1 h at room temperature. Then the PVDF membranes were immunoblotted overnight with primary monoclonal antibodies against either β-Actin at 1:200 dilution or ABCB1 or ABCG2 at 1:200 dilution at 4°C, and were then further incubated for 2 h at room temperature with rabbit anti-mouse horseradish peroxide (HRP)-conjugated secondary antibody (1:2000 dilution). The protein–antibody complex was detected by enhanced chemiluminescence detection system (Amersham, NJ). β-Actin was used to confirm equal loading in each lane in the samples prepared from cell lysates. The protein expression was quantified by ImageJ 1.47v Software (NIH, USA).

2.8. Immunofluorescence

Cells (1 × 10^4) were seeded in 96-well plate and harvested overnight. After treating with motesanib at 3 μM for 72 h, cells were washed with PBS and fixed with 4% paraformaldehyde for 15 min at room temperature and then rinsed with PBS three times. Then cells were kept in 1% Triton X-100 for 10 min at 4°C and rinsed with PBS three times. Non-specific reaction was blocked with BSA (2 mg/ml) for 1 h at 37°C. The monoclonal antibody against ABCB1 (P7965) (1:200) (Sigma Chemical Co., St. Louis, MO) was applied overnight, followed by an Alexa flour 488-conjugated goat anti-mouse IgG (1:100)

(Molecular Probes, Eugene, OR) for 1 h. DAPI was used to counterstain the nuclei. Images were taken with an inverted IX70 microscope (Olympus, Center Valley, PA) with IX-FLA fluorescence and CCD camera.

2.9. ABCB1 ATPase assay

The vanadate-sensitive ATPase activity of ABCB1 in crude membranes of High-five insect cells, in the presence of concentrations of motesanib ranging from 0 to 40 μM, was measured as previously described [46].

2.10. Molecular modeling – ABCB1

Motesanib structure was built for docking simulation into human ABCB1 following the same protocol as previously described [47]. The refined crystal structure of mouse ABCB1 in complex with QZ59-RRR (PDB ID: 4M2S) [48] and QZ59-SSS (PDB ID: 4M2T) [48] as the template obtained from the RCSB Protein Data Bank were used to generate the drug-bound homology model of the human ABCB1. Homology modeling was carried out using the default parameters of Prime v3.3 as implemented in Maestro v9.5 (Schrödinger, LLC, New York, NY, 2013) essentially as reported previously [49]. ABCB1 homology models with bound QZ59-RRR and QZ59-SSS inhibitors were used to generate docking grids for site-1 and site-2, respectively [50]. Homology model of ABCB1 based on the corrected mouse ABCB1 crystal structure in apoprotein state was provided by S. Aller and it was used to generate docking grids for site-3 and site-4 [51]. Glide v6.0 (Schrödinger, LLC, New York, NY, 2013) docking protocol was followed with the default functions to dock motesanib at each of the drug-binding sites. Top scoring conformation of motesanib was used for graphical analysis. All computations were carried out on a Dell Precision 490n dual processor with Linux OS (Ubuntu 12.04 LTS).

2.11. Statistical analysis

All experiments were repeated at least three times and the differences were determined by using the Student's t-test. The statistical significance was determined at $P < 0.05$.

3. Results

3.1. Effect of motesanib on ABCB1 substrates in cell lines overexpressing ABCB1

In order to select a non-toxic drug concentration for motesanib, cytotoxicity assays were performed on the cell lines (Fig. 1B, C). Based on these results, concentrations of 1 μM and 3 μM were chosen, because more than 85% of the cells survived at 3 μM. In order to determine whether motesanib could reverse ABCB1-mediated MDR, cell survival assays were performed in the presence and absence of motesanib, using the parental KB-3-1 cell line and drug selective KB-C2 cell line. The drug selective KB-C2 cell line showed 260.0-, 237.3- and 132.8-fold resistance to paclitaxel, colchicine and vincristine (all substrates of ABCB1), respectively, as compared to the parental KB-3-1 cell line. However, there was no significant difference in the response of KB-3-1 and KB-C2 cells to cisplatin, which is not a substrate of ABCB1. Motesanib, at 1 μM and 3 μM, significantly decreased the resistance of paclitaxel, colchicine and vincristine in KB-C2 cells compared to KB-3-1 cells, whose resistance was not significantly altered by motesanib (Table 1). This reversal effect was

similar to the one obtained when using verapamil at 3 μM. No significant change was observed in the IC_{50} for KB-3-1 and KB-C2 when 3 μM motesanib or verapamil was used as inhibitor in combination with cisplatin, which is not a substrate of ABCB1.

However, there could be multiple factors responsible for the development of MDR in cancer cells [52,53]. In order to limit those factors to only one modulated by ABCB1, we used ABCB1-transfected cell line LLC-MDR1-WT and parental cell line LLC-PK1 [41]. The LLC-MDR1-WT was 41.1-fold resistant to paclitaxel as compared to LLC-PK1. However, there was no significant difference in the IC_{50} values of cisplatin in LLC-PK1 and LLC-MDR1-WT cells. Motesanib, at 1 μM and 3 μM, produced a concentration-dependent decrease in ABCB1-mediated resistance to paclitaxel (Table 1). We also used verapamil as a positive control and obtained the similar results. In addition, 3 μM of motesanib or verapamil did not significantly alter the IC_{50} values for cisplatin (which is not a substrate of ABCB1 transporter) in both LLC-PK1 and LLC-MDR1-WT cell lines. These results suggest that motesanib has the strong capability to enhance the sensitivity of ABCB1 substrates in both drug selected and transfected cell lines overexpressing ABCB1.

3.2. Effect of motesanib on cell lines overexpressing ABCG2, ABCC1 and ABCC10

In order to determine the effect of motesanib on the ABCG2 transporter, we used parental cell line NCI-H460 and drug selected cell line NCI-H460/MX20 overexpressing ABCG2. The incubation of NCI-H460/MX20 cells with mitoxantrone produced a 135.4-fold resistance to mitoxantrone as compared to the parental cell line NCI-H460. However, there was no significant difference in the response of NCI-H460 and NCI-H460/MX20 cells to cisplatin, which is not a substrate of ABCG2 transporter. The incubation of cells with 3 μM of motesanib, in combination with mitoxantrone, moderately decreased the resistance to 47.0-fold as compared to the parental NCI-H460 cell line, whose drug sensitivity was not significantly altered by motesanib (Table 2). FTC was used as a positive control for ABCG2 inhibition and the results showed that FTC (3 μM) significantly decreased the resistance of NCI-H460/MX20 cells to mitoxantrone to 4.1-fold as compared to NCI-H460 cells. There was no significant alteration in the IC_{50} values of NCI-H460 and NCI-H460/MX20 when motesanib or FTC at 3 μM was used as inhibitors in combination with cisplatin, which is not a substrate of ABCG2. Therefore, motesanib could partially reverse ABCG2-mediated MDR.

Then we used parental HEK293/pcDNA3.1 and ABCC1 transfected HEK/ABCC1 cells to determine if motesanib could reverse ABCC1-mediated MDR. The 1.5 μM was chosen as a non-toxic concentration for motesanib, because more than 85% of these cells survived at 1.5 μM (Fig. 1E). As shown in Table 3, HEK/ABCC1 cells were 27.7-fold resistant to vincristine as compared to HEK293/pcDNA3.1 cells. Motesanib (1.5 μM) did not significantly alter the IC_{50} values of HEK293/pcDNA3.1 and HEK/ABCC1 cells to vincristine. We used PAK-104P as a positive control inhibitor of ABCC1 and the results suggested that PAK-104P at 2.5 μM significantly decreased the resistance of HEK/ABCC1 to vincristine to 5.3-fold as compared to parental HEK293/pcDNA3.1 cells (Table 3). Collectively, motesanib did not significantly reverse ABCC1-mediated MDR. Furthermore, we used parental HEK293/pcDNA3.1 and ABCC10 transfected HEK/ABCC10 cells to

study the effect of motesanib on ABCC10. The 1.5 μM was chosen as a non-toxic concentration for motesanib, because more than 85% of these cells survived at 1.5 μM (Fig. 1F). The results indicated that HEK/ABCC10 cells were 9.2-fold resistant to paclitaxel as compared to HEK293/pcDNA3.1 cells. Motesanib (1.5 μM) did not significantly alter the IC_{50} values of HEK293/pcDNA3.1 and HEK/ABCC10 cells to paclitaxel. We used cepharanthine as a positive control inhibitor of ABCC10 and the results indicated that cepharanthine at 2.5 μM significantly decreased the resistance of HEK/MRP7 to paclitaxel to 1.1-fold as compared to parental HEK293/pcDNA3.1 cells (Table 3). In conclusion, motesanib cannot significantly reverse ABCC10-mediated MDR.

3.3. Effect of motesanib on cellular accumulation of [^{3}H]-paclitaxel

Although the results of the cell survival assay suggest that motesanib reverse MDR that is regulated by ABCB1 transporter, they do not explain what the mechanism of this action is inside the cells. Therefore, we performed the drug accumulation assay to elucidate the mechanism of action. [^{3}H]-paclitaxel, a substrate of ABCB1 transporter, was incubated with motesanib in parental KB-3-1 cells and drug selected KB-C2 cells to determine its intracellular accumulation. The incubation of KB-C2 cells with 1 μM and 3 μM motesanib significantly increased the intracellular accumulation of [^{3}H]-paclitaxel in a concentration-dependent manner as compared to the parental KB-3-1 cells (Fig. 2A). In addition, the results were comparable to those obtained by incubating KB-3-1 and KB-C2 cells with verapamil (3 μM), which is a known inhibitor of ABCB1 transporter.

3.4. Motesanib inhibits the efflux activity of ABCB1 transporter

To ascertain whether motesanib can directly inhibit the efflux activity of ABCB1, further leading to the increase in the intracellular accumulation of [^{3}H]-paclitaxel, we tested the efflux of [^{3}H]-paclitaxel with or without motesanib at different time points (0, 30, 60, 120 min) in ABCB1 overexpressing cells. The remaining intracellular amount of [^{3}H]-paclitaxel of KB-C2 cells was significantly lower compared to that of parental KB-3-1 cells due to active transport of the [^{3}H]-paclitaxel by the ABCB1 transporter. However, motesanib (3 μM) significantly decreased the efflux of [^{3}H]-paclitaxel by blocking the efflux function of ABCB1 transporter (Fig. 2B). Similarly, verapamil (3 μM) significantly decreased the efflux of [^{3}H]-paclitaxel.

3.5. Effect of motesanib on the expression levels of ABCB1 and ABCG2

Western blot analysis indicated a band with a molecular weight of approximately 170-kDa in the KB-C2 cell lysates, suggesting the presence of ABCB1 protein. In contrast, this band was not present in parental KB-3-1, indicating the absence of ABCB1 protein (Fig. 3A, C). A protein expression band with higher intensity of molecular weight of 72-kDa was present in the NCI-H460/MX20 cell lysates, suggesting the high expression level of ABCG2 protein in this cell line. However, the expression level of this band was much lower in the parental NCI-H460 cell line, indicating a low expression level of ABCG2 in this cell line as compared to that in the NCI-H460/MX20 cell line (Fig. 3B, D).

To confirm that the reversal of ABCB1- and ABCG2-mediated MDR by motesanib was not due to a decrease in the protein expression levels, we determined the effect of incubating

cells with motesanib (3 μM) for 0, 24, 48 and 72 h. Subsequently, we measured the expression levels of ABCB1 and ABCG2 in the respective cell lysates. There was no significant change in the expression levels of the ABCB1 protein in the KB-C2 cells (Fig. 3A, C). Furthermore, the expression level of the ABCG2 protein was not significantly altered in the NCI-H460/MX20 cells (Fig. 3B, D). These findings revealed that the reversal of MDR by motesanib was not due to a decrease in protein expression, but resulted from an increase in intracellular accumulation of chemotherapeutic drugs.

3.6. Motesanib does not alter the localization of ABCB1 and ABCG2

Presumably, the transporters could be down regulated, if they are translocated or dislodged from plasma membrane to cytosolic region. To rule out this possibility, we performed an immunofluorescence assay to examine whether the location of ABCB1 and ABCG2 was altered after the treatment with motesanib. As shown in Fig. 4A and 4B, there was no alteration of ABCB1 and ABCG2 protein localization in plasma membranes after the treatment with motesanib at 3 μM for 72 h. The Western blot analysis (Fig. 3) and immunofluorescence assay (Fig. 4A, B) suggested that motesanib did not significantly change the expression and localization of the ABCB1 in KB-C2 cells and those of ABCG2 in NCI-H460/MX20 cells.

3.7. Effect of motesanib on the ABCB1 ATP hydrolysis

ABCB1 transporter utilizes energy derived from the hydrolysis of ATP to efflux their substrates across the membrane against a concentration gradient, thus ATP consumption reflects its ATPase activity. To assess the effect of motesanib on the ATPase activity of ABCB1, we measured ABCB1-mediated ATP hydrolysis in the presence of motesanib at various concentrations from 0 to 40 μM. Similar to other TKIs, motesanib stimulated the ATPase activity of ABCB1 in a concentration dependent manner, with a maximal stimulation of 2.29-fold of the basal activity (Fig. 4C). The inset in Fig. 4C demonstrates that the concentration of motesanib required to obtain 50% stimulation is 0.893 μM. The result suggested that motesanib interacts at the drug-substrate-binding site and affects the ATPase activity of ABCB1.

3.8. Docking analysis of motesanib with human ABCB1 homology model

To understand the binding interaction of motesanib with the homology model of human ABCB1 [54], docking studies were performed on site-1 to site-4 of ABCB1. The Glide docking score (site-1: −8.2 kcal/mol, site-2: −8.3 kcal/mol, site-3: −8.0 kcal/mol, and site-4: −8.3 kcal/mol) showed that motesanib may bind to all transmembrane drug-binding sites of ABCB1 due to exceptional flexibility and large drug-binding site present in ABCB1 [55]. According to these scores, we considered site-4 (a common site) for discussion of motesanib binding interactions (Fig. 5).

The pyridine-4-yl-methyl amino group of motesanib formed hydrophobic contacts with the hydrophobic pocket lined with residues Met68, Met69, Phe72, Tyr118, Tyr953, Phe957 and Phe978. The nicotinamide group was also involved in hydrophobic contacts with the side chains of Leu65, Phe336, Ile340, Phe983 and Met986. Moreover, the N1 atom of nicotinamide group formed a hydrogen bond with the hydroxyl group of Tyr953(-N•••HO-

Tyr953, 2.2 Å). The 3,3-dimethyl-2,3-dihydro-1*H*-indol-6-yl group bound in a pocket surrounded by Ile306, Tyr307, Tyr310, Gln725 and Phe728.

4. Discussion

ABCB1/P-gp developed as such an essential MDR transporter along with some relatively novel transporters (like ABCG2, ABCC1 and ABCC10) family for several major chemotherapeutic drugs. Widespread expression of ABCB1 and ABCG2 in prominent body organs has not only protective function against some xenobiotics and pharmacological compounds, but also affects the pharmacokinetics of some substrate chemotherapeutic drugs [56]. Development of TKIs in recent years has marked a therapeutic breakthrough in cancer treatment. Several small molecule TKIs have recently been approved for some types of cancer treatment, including imatinib, gefitinib, erlotinib, sunitinib, dasatinib, sorafenib and lapatinib [57]. All of these small molecule TKIs have shown clinical application in a variety of cancers that are highly resistant to conventional chemotherapeutic agents, including mast cell disease, different forms of leukemia, sarcomas, hypereosinophilic syndrome, breast, hepatocellular carcinoma, renal and lung cancer. As the new TKIs are being brought into the clinic, a great deal of effort will be aimed at increasing the anticancer activity of conventional chemotherapeutic agents or restoring the chemosensitivity of refractory and resistant cancer cells to conventional chemotherapeutic agents.

One of the major findings of this study was that motesanib significantly increased the sensitivity of ABCB1 overexpressing KB-C2 drug selected cell line to paclitaxel, colchicine and vincristine, which are substrates of ABCB1 transporter. The motesanib-induced enhancement in the sensitivity of KB-C2 cells to the substrates was represented by a significant decrease in the IC_{50} values for the aforementioned substrates in the presence of motesanib in the MTT assay, a measurement of cell survival (Table 1). The motesanib-induced potentiation was selective because at the concentrations used in this study (1 μM and 3 μM), motesanib (1) did not produce a significant toxic effect on the parental KB-3-1 cell (non-overexpressing) and (2) failed to potentiate the effect of the substrate drugs on the parental KB-3-1 cells. Importantly, the concentrations we used in this study were lower than the range of the maximal plasma concentration (2.10 ± 1.41 μM) obtained in the clinical trials of motesanib diphosphate in progressive differentiated thyroid cancer [32]. In addition, motesanib did not significantly potentiate the toxic effect of cisplatin, which is not a substrate of ABCB1 transporter, and this finding further supports the specificity of motesanib. Verapamil (3 μM), a known inhibitor of ABCB1 transporter, also significantly potentiated the toxic effect of paclitaxel, colchicine and vincristine on KB-C2 cells. Moreover, verapamil did not potentiate the toxic effect of cisplatin on the parental KB-3-1 or KB-C2 cells. Therefore, motesanib is an inhibitor of the ABCB1 transporter in ABCB1 overexpressing KB-C2 drug selected cells.

We also determined the effect of motesanib on ABCB1 substrates in ABCB1-transfected cell lines. Motesanib, at 1 μM and 3 μM, produced a concentration-dependent decrease in ABCB1-mediated resistance to paclitaxel in ABCB1 overexpressing LLC-MDR1-WT transfected cell line (Table 1). This study also tested the effect of motesanib on the sensitivity of ABCC1 overexpressing HEK/ABCC1 transfected cells to vincristine and

ABCC10 overexpressing HEK/ABCC10 transfected cells to paclitaxel. Motesanib did not significantly alter the IC_{50} values of vincristine in HEK/ABCC1 and paclitaxel in HEK/ABCC10 cell line (Table 3). In contrast, PAK-104P, as a known inhibitor of ABCC1, significantly reversed the ABCC1-mediated MDR. The incubation of HEK/ABCC10 cells with cepharanthine, which is a known inhibitor of ABCC10 transporter, significantly increased the sensitivity of the transfected cells to paclitaxel [58]. These results suggest that the motesanib-induced potentiation of the toxic effects of ABCB1 substrates on ABCB1 overexpressing cells is not due to its interaction with the ABCC1 and ABCC10 transporter.

Another major finding of this study was that *in vitro*, motesanib (3 μM) significantly enhanced the sensitivity of ABCG2 overexpressing MDR cells NCI-H460/MX20 to mitoxantrone, which is a substrate of the ABCG2 transporter. This effect was manifested by motesanib producing a significant decrease in the IC_{50} values of the substrate drugs in the MTT assay. In contrast, motesanib did not significantly alter the IC_{50} values for the aforementioned substrate drugs in parental NCI-H460 cells. Furthermore, motesanib did not alter the sensitivity of NCI-H460/MX20 cell line to cisplatin, which is not a substrate for ABCG2. These results show that in addition to inhibiting the ABCB1 transporter, motesanib partially reverses ABCG2-mediated MDR.

Although our findings suggest that motesanib could re-sensitize ABCB1 overexpressing cells to substrate drugs, these still cannot explain its mechanism of action. Hence, we conducted experiments to ascertain if motesanib affected the intracellular accumulation and efflux of [^{3}H]-paclitaxel, which is a substrate of the ABCB1. Motesanib and verapamil (a known ABCB1 inhibitor) produced a significant increase in the intracellular accumulation of [^{3}H]-paclitaxel in ABCB1 overexpressing KB-C2 cell line. Furthermore, motesanib and verapamil significantly decreased the efflux of [^{3}H]-paclitaxel from KB-C2 cells. These findings suggested that motesanib sensitized ABCB1 overexpressing cells to paclitaxel (and potentially other substrate drugs) by inhibiting the efflux function of ABCB1 transporter.

It is conceivable that motesanib could increase the sensitivity of KB-C2 cells to paclitaxel, colchicine and vincristine through a decrease in the expression levels of ABCB1, i.e. there are fewer transporters and it would lead to an enhancement in intracellular drug accumulation. This is unlikely as the incubation of cells with motesanib (3 μM for 0, 24, 48, 72 h) did not significantly alter the expression level of ABCB1 in KB-C2 cells (Fig. 3A, C). Additionally, there was no expression of ABCB1 protein at the 170-kDa position in parental KB-3-1 cells, indicating that these cells do not express ABCB1. This finding is consistent with our results showing that there is no significant alteration in the sensitivity of parental KB-3-1 cells to ABCB1 substrate drugs in the presence of motesanib. Furthermore, the expression level of ABCG2 was not significantly altered in the NCI-H460/MX20 cells (Fig. 3B, D). In the Western blot analysis, we used the whole cell lysates. Therefore, one cannot rule out the possibility that motesanib reduces the insertion of the ABCB1 and ABCG2 transporters into the cell membrane. This effect could lead to an enhancement in the sensitivity of KB-C2 and NCI-H460/MX20 cells to respective substrate drugs as fewer ABCB1 and ABCG2 transporters would be present in the cell membrane. Thus, we performed an immunofluorescence assay to examine whether the location of ABCB1 and ABCG2 was altered after the treatment with motesanib. As shown in Fig. 4A and 4B, there

was no significant alteration of ABCB1 and ABCG2 protein localization in plasma membranes after the treatment with motesanib (3 μM) for 72 h. Furthermore, motesanib stimulated the ATPase activity of ABCB1 in a concentration dependent manner, with a maximal stimulation of 2.29-fold of the basal activity (Fig. 4C).

In order to further study the interaction between motesanib and ABCB1 transporter, we conducted the docking analysis of motesanib with human ABCB1 homology model (Fig. 5). Due to the absence of co-crystal structures of human ABCB1, our docking studies were based on homology model of human ABCB1 developed using recently published corrected mouse ABCB1 crystal structure [48]. Motesanib is comprised of required pharmacophoric groups, such as hydrophobic groups and/or aromatic ring centers (3,3-dimethyl-2,3-dihydroindole and pyridine ring), hydrogen-bond acceptors and hydrogen-bond donor groups (pyridine ring nitrogen, indole -NH and carboxamide) that have been described important for interaction with the drug-binding cavity of ABCB1 transporters [59]. Moreover, motesanib is reasonably hydrophobic as evident from calculated logP value of 3.5. Overall, these docking results may be useful to understand ligand-protein interactions and to provide clues for further optimization of motesanib.

So far, this is the first study to report that motesanib significantly reverses MDR mediated by the overexpression of the ABCB1 transporter. Previously, it has been reported that small TKIs, including erlotinib [60], nilotinib [20], lapatinib [22], sunitinib [26], dasatinib [61], gefitinib [62] and apatinib [63] can reverse MDR in cell lines by competitively inhibiting the efflux of the substrate drugs from the cells. Motesanib is currently under Phase II and Phase III clinical trials for advanced gastrointestinal stromal tumor (GIST), fallopian tube cancer, ovarian cancer, thyroid cancer, non-small lung cancer (www.clinicaltrials.gov). In conclusion, motesanib is one of the most promising reversal agent as compared to all TKIs characterized so far in MDR mediated by ABC transporters, most likely by blocking its function. Furthermore, the clinical trials of motesanib alone and in combination with other chemotherapeutic drugs are ongoing. Hopefully, this study would be helpful in determining potential pharmacokinetic interactions of motesanib when selected with other combinational therapies, in the context of ABCB1-mediated MDR and prove clinically useful.

Acknowledgments

Abbreviations

MDR	multidrug resistance
ABC	ATP-binding cassette
ABCB1	ABC transporter subfamily B member 1

ABCG2	ABC transporter subfamily G member 2
VEGFR	vascular endothelial growth factor receptor
TKI	tyrosine kinase inhibitor

References

1. Siegel R, Ward E, Brawley O, Jemal A. Cancer statistics, 2011: The impact of eliminating socioeconomic and racial disparities on premature cancer deaths. Ca : a Cancer Journal for Clinicians. 2011; 61:212. [PubMed: 21685461]

2. Jemal A, Murray T, Ward E, Samuels A, Tiwari RC, Ghafoor A, et al. Cancer statistics, 2005. CA Cancer. J. Clin. 2005; 55:10–30. [PubMed: 15661684]

3. Gottesman MM. Mechanisms of cancer drug resistance. Annu. Rev. Med. 2002; 53:615–627. [PubMed: 11818492]

4. Quintieri L, Fantin M, Vizler C. Identification of molecular determinants of tumor sensitivity and resistance to anticancer drugs. Adv. Exp. Med. Biol. 2007; 593:95–104. [PubMed: 17265720]

5. Dean M, Allikmets R. Complete characterization of the human ABC gene family. J. Bioenerg. Biomembr. 2001; 33:475–479. [PubMed: 11804189]

6. Deeley RG, Westlake C, Cole SP. Transmembrane transport of endo- and xenobiotics by mammalian ATP-binding cassette multidrug resistance proteins. Physiol. Rev. 2006; 86:849–899. [PubMed: 16816140]

7. Dean M, Annilo T. Evolution of the ATP-binding cassette (ABC) transporter superfamily in vertebrates. Annu. Rev. Genomics Hum. Genet. 2005; 6:123–142. [PubMed: 16124856]

8. Juliano RL, Ling V. A surface glycoprotein modulating drug permeability in Chinese hamster ovary cell mutants. Biochim. Biophys. Acta. 1976; 455:152–162. [PubMed: 990323]

9. Schinkel AH, Mol CA, Wagenaar E, van Deemter L, Smit JJ, Borst P. Multidrug resistance and the role of P-glycoprotein knockout mice. Eur. J. Cancer. 1995; 31A:1295–1298. [PubMed: 7577039]

10. Gottesman MM, Fojo T, Bates SE. Multidrug resistance in cancer: role of ATP-dependent transporters. Nat. Rev. Cancer. 2002; 2:48–58. [PubMed: 11902585]

11. Sarkadi B, Homolya L, Szakacs G, Varadi A. Human multidrug resistance ABCB and ABCG transporters: participation in a chemoimmunity defense system. Physiol. Rev. 2006; 86:1179–1236. [PubMed: 17015488]

12. Roskoski R Jr. STI-571: an anticancer protein-tyrosine kinase inhibitor. Biochem. Biophys. Res. Commun. 2003; 309:709–717. [PubMed: 13679030]

13. Litman T, Brangi M, Hudson E, Fetsch P, Abati A, Ross DD, et al. The multidrug-resistant phenotype associated with overexpression of the new ABC half-transporter, MXR (ABCG2). J. Cell. Sci. 2000; 113(Pt 11):2011–2021. [PubMed: 10806112]

14. Mao Q, Unadkat JD. Role of the breast cancer resistance protein (ABCG2) in drug transport. AAPS J. 2005; 7:E118–E133. [PubMed: 16146333]

15. Kruh GD, Belinsky MG. The MRP family of drug efflux pumps. Oncogene. 2003; 22:7537–7552. [PubMed: 14576857]

16. Sodani K, Patel A, Kathawala RJ, Chen ZS. Multidrug resistance associated proteins in multidrug resistance. Chin. J. Cancer. 2012; 31:58–72. [PubMed: 22098952]

17. Hopper-Borge EA, Churchill T, Paulose C, Nicolas E, Jacobs JD, Ngo O, et al. Contribution of Abcc10 (Mrp7) to in vivo paclitaxel resistance as assessed in Abcc10(−/−) mice. Cancer Res. 2011; 71:3649–3657. [PubMed: 21576088]

18. Kathawala RJ, Wang YJ, Ashby CR Jr, Chen ZS. Recent advances regarding the role of ABC subfamily C member 10 (ABCC10) in the efflux of antitumor drugs. Chin. J. Cancer. 2013

19. Shukla S, Chen ZS, Ambudkar SV. Tyrosine kinase inhibitors as modulators of ABC transporter-mediated drug resistance. Drug Resist Updat. 2012; 15:70–80. [PubMed: 22325423]

20. Tiwari AK, Sodani K, Wang SR, Kuang YH, Ashby CR Jr, Chen X, et al. Nilotinib (AMN107, Tasigna) reverses multidrug resistance by inhibiting the activity of the ABCB1/Pgp and ABCG2/BCRP/MXR transporters. Biochem. Pharmacol. 2009; 78:153–161. [PubMed: 19427995]

21. Ozvegy-Laczka C, Cserepes J, Elkind NB, Sarkadi B. Tyrosine kinase inhibitor resistance in cancer: role of ABC multidrug transporters. Drug Resist Updat. 2005; 8:15–26. [PubMed: 15939339]

22. Dai CL, Tiwari AK, Wu CP, Su XD, Wang SR, Liu DG, et al. Lapatinib (Tykerb, GW572016) reverses multidrug resistance in cancer cells by inhibiting the activity of ATP-binding cassette subfamily B member 1 and G member 2. Cancer Res. 2008; 68:7905–7914. [PubMed: 18829547]

23. Kuang Y, Shen T, Chen X, Sodani K, Hopper-Borge E, Tiwari AK, et al. Lapatinib and erlotinib are potent reversal agents for MRP7 (ABCC10)-mediated multidrug resistance. Biochem. Pharmacol. 2010; 79:154–161. [PubMed: 19720054]

24. Shen T, Kuang Y, Ashby CR, Lei Y, Chen A, Zhou Y, et al. Imatinib and Nilotinib Reverse Multidrug Resistance in Cancer Cells by Inhibiting the Efflux Activity of the MRP7 (ABCC10). PLoS One. 2009; 4 n/a.

25. Erlichman C, Boerner SA, Hallgren CG, Spieker R, Wang XY, James CD, et al. The HER tyrosine kinase inhibitor CI1033 enhances cytotoxicity of 7-ethyl-10-hydroxycamptothecin and topotecan by inhibiting breast cancer resistance protein-mediated drug efflux. Cancer Res. 2001; 61:739–748. [PubMed: 11212277]

26. Dai CL, Liang YJ, Wang YS, Tiwari AK, Yan YY, Wang F, et al. Sensitization of ABCG2-overexpressing cells to conventional chemotherapeutic agent by sunitinib was associated with inhibiting the function of ABCG2. Cancer Lett. 2009; 279:74–83. [PubMed: 19232821]

27. Shukla S, Robey RW, Bates SE, Ambudkar SV. Sunitinib (Sutent, SU11248), a small-molecule receptor tyrosine kinase inhibitor, blocks function of the ATP-binding cassette (ABC) transporters P-glycoprotein (ABCB1) and ABCG2. Drug Metab. Dispos. 2009; 37:359–365. [PubMed: 18971320]

28. Polverino A, Coxon A, Starnes C, Diaz Z, DeMelfi T, Wang L, et al. AMG 706, an oral, multikinase inhibitor that selectively targets vascular endothelial growth factor, platelet-derived growth factor, and kit receptors, potently inhibits angiogenesis and induces regression in tumor xenografts. Cancer Res. 2006; 66:8715–8721. [PubMed: 16951187]

29. Coxon A, Bush T, Saffran D, Kaufman S, Belmontes B, Rex K, et al. Broad antitumor activity in breast cancer xenografts by motesanib, a highly selective, oral inhibitor of vascular endothelial growth factor, platelet-derived growth factor, and Kit receptors. Clin. Cancer Res. 2009; 15:110–118. [PubMed: 19118038]

30. Coxon A, Ziegler B, Kaufman S, Xu M, Wang H, Weishuhn D, et al. Antitumor activity of motesanib alone and in combination with cisplatin or docetaxel in multiple human non-small-cell lung cancer xenograft models. Mol. Cancer. 2012; 11 70,4598-11-70.

31. Benjamin RS, Schoffski P, Hartmann JT, Van Oosterom A, Bui BN, Duyster J, et al. Efficacy and safety of motesanib, an oral inhibitor of VEGF, PDGF, and Kit receptors, in patients with imatinib-resistant gastrointestinal stromal tumors. Cancer Chemother. Pharmacol. 2011; 68:69–77. [PubMed: 20838998]

32. Sherman SI, Wirth LJ, Droz J, Hofmann M, Bastholt L, Martins RG, et al. Motesanib Diphosphate in Progressive Differentiated Thyroid Cancer. N. Engl. J. Med. 2008; 359:31–42. [PubMed: 18596272]

33. Schlumberger MJ, Elisei R, Bastholt L, Wirth LJ, Martins RG, Locati LD, et al. Phase II study of safety and efficacy of motesanib in patients with progressive or symptomatic, advanced or metastatic medullary thyroid cancer. J. Clin. Oncol. 2009; 27:3794–3801. [PubMed: 19564535]

34. Kubota K, Ichinose Y, Scagliotti G, Spigel D, Kim JH, Shinkai T, et al. Phase III study (MONET1) of motesanib plus carboplatin/paclitaxel in patients with advanced nonsquamous nonsmall-cell lung cancer (NSCLC): Asian subgroup analysis. Ann. Oncol. 2014; 25:529–536. [PubMed: 24419239]

35. Matsuo K, Eno ML, Ahn EH, Shahzad MM, Im DD, Rosenshein NB, et al. Multidrug resistance gene (MDR-1) and risk of brain metastasis in epithelial ovarian, fallopian tube, and peritoneal cancer. Am. J. Clin. Oncol. 2011; 34:488–493. [PubMed: 20921883]

36. Eechoute K, Sparreboom A, Burger H, Franke RM, Schiavon G, Verweij J, et al. Drug transporters and imatinib treatment: implications for clinical practice. Clin. Cancer Res. 2011; 17:406–415. [PubMed: 21163869]

37. Gao YJ, Li B, Wu XY, Cui J, Han JK. Thyroid tumor-initiating cells: increasing evidence and opportunities for anticancer therapy (review). Oncol. Rep. 2014; 31:1035–1042. [PubMed: 24424445]

38. Gao B, Russell A, Beesley J, Chen XQ, Healey S, Henderson M, et al. Paclitaxel sensitivity in relation to ABCB1 expression, efflux and single nucleotide polymorphisms in ovarian cancer. Sci. Rep. 2014; 4:4669. [PubMed: 24810093]

39. Han JY, Lim HS, Yoo YK, Shin ES, Park YH, Lee SY, et al. Associations of ABCB1, ABCC2, and ABCG2 polymorphisms with irinotecan-pharmacokinetics and clinical outcome in patients with advanced non-small cell lung cancer. Cancer. 2007; 110:138–147. [PubMed: 17534875]

40. Akiyama S, Fojo A, Hanover J, Pastan I, Gottesman MM. Isolation and genetic characterization of human KB cell lines resistant to multiple drugs. Somat. Cell Mol. Genet. 1985; 11:117–126. [PubMed: 3856953]

41. Fung KL, Pan J, Ohnuma S, Lund PE, Pixley JN, Kimchi-Sarfaty C, et al. MDR1 synonymous polymorphisms alter transporter specificity and protein stability in a stable epithelial monolayer. Cancer Res. 2014; 74:598–608. [PubMed: 24305879]

42. Zhang H, Wang YJ, Zhang YK, Wang DS, Kathawala RJ, Patel A, et al. AST1306, a potent EGFR inhibitor, antagonizes ATP-binding cassette subfamily G member 2-mediated multidrug resistance. Cancer Lett. 2014

43. Chen ZS, Hopper-Borge E, Belinsky MG, Shchaveleva I, Kotova E, Kruh GD. Characterization of the transport properties of human multidrug resistance protein 7 (MRP7, ABCC10). Mol. Pharmacol. 2003; 63:351–358. [PubMed: 12527806]

44. Carmichael J, DeGraff WG, Gazdar AF, Minna JD, Mitchell JB. Evaluation of a tetrazolium-based semiautomated colorimetric assay: assessment of chemosensitivity testing. Cancer Res. 1987; 47:936–942. [PubMed: 3802100]

45. Sodani K, Tiwari AK, Singh S, Patel A, Xiao Z, Chen J, et al. GW583340 and GW2974, human EGFR and HER-2 inhibitors, reverse ABCG2- and ABCB1-mediated drug resistance. Biochem. Pharmacol. 2012; 83:1613–1622. [PubMed: 22414725]

46. Ambudkar SV. Drug-stimulatable ATPase activity in crude membranes of human MDR1-transfected mammalian cells. Methods Enzymol. 1998; 292:504–514. [PubMed: 9711578]

47. Kathawala RJ, Chen JJ, Zhang YK, Wang YJ, Patel A, Wang DS, et al. Masitinib antagonizes ATP-binding cassette subfamily G member 2-mediated multidrug resistance. Int. J. Oncol. 2014; 44:1634–1642. [PubMed: 24626598]

48. Li J, Jaimes KF, Aller SG. Refined structures of mouse P-glycoprotein. Protein Sci. 2014; 23:34–46. [PubMed: 24155053]

49. Ding PR, Tiwari AK, Ohnuma S, Lee JW, An X, Dai CL, et al. The phosphodiesterase-5 inhibitor vardenafil is a potent inhibitor of ABCB1/P-glycoprotein transporter. PLoS One. 2011; 6:e19329. [PubMed: 21552528]

50. Shi Z, Tiwari AK, Shukla S, Robey RW, Singh S, Kim IW, et al. Sildenafil reverses ABCB1- and ABCG2-mediated chemotherapeutic drug resistance. Cancer Res. 2011; 71:3029–3041. [PubMed: 21402712]

51. Guo HQ, Zhang GN, Wang YJ, Zhang YK, Sodani K, Talele TT, et al. beta-Elemene, a compound derived from Rhizoma zedoariae, reverses multidrug resistance mediated by the ABCB1 transporter. Oncol. Rep. 2014; 31:858–866. [PubMed: 24284783]

52. Calcagno AM, Ambudkar SV. Molecular mechanisms of drug resistance in single-step and multi-step drug-selected cancer cells. Methods Mol. Biol. 2010; 596:77–93. [PubMed: 19949921]

53. Calcagno AM, Fostel JM, To KK, Salcido CD, Martin SE, Chewning KJ, et al. Single-step doxorubicin-selected cancer cells overexpress the ABCG2 drug transporter through epigenetic changes. Br. J. Cancer. 2008; 98:1515–1524. [PubMed: 18382425]

54. Aller SG, Yu J, Ward A, Weng Y, Chittaboina S, Zhuo R, et al. Structure of P-glycoprotein reveals a molecular basis for poly-specific drug binding. Science. 2009; 323:1718–1722. [PubMed: 19325113]

55. Ferreira RJ, Ferreira MJ, dos Santos DJ. Molecular docking characterizes substrate-binding sites and efflux modulation mechanisms within P-glycoprotein. J. Chem. Inf. Model. 2013; 53:1747–1760. [PubMed: 23802684]

56. Allen JD, van Loevezijn A, Lakhai JM, van der Valk M, van Tellingen O, Reid G, et al. Potent and specific inhibition of the breast cancer resistance protein multidrug transporter in vitro and in mouse intestine by a novel analogue of fumitremorgin C. Mol. Cancer. Ther. 2002; 1:417–425. [PubMed: 12477054]

57. Polli JW, Humphreys JE, Harmon KA, Castellino S, O'Mara MJ, Olson KL, et al. The role of efflux and uptake transporters in [N-{3-chloro-4-[(3-fluorobenzyl)oxy]phenyl}-6-[5-({[2-(methylsulfonyl)ethyl]amino }m ethyl)-2-furyl]-4-quinazolinamine (GW572016, lapatinib) disposition and drug interactions. Drug Metab. Dispos. 2008; 36:695–701. [PubMed: 18216274]

58. Zhou Y, Hopper-Borge E, Shen T, Huang X, Shi Z, Kuang Y, et al. Cepharanthine is a potent reversal agent for MRP7(ABCC10)-mediated multidrug resistance. Biochem. Pharmacol. 2009; 77:993–1001. [PubMed: 19150344]

59. Klepsch F, Jabeen I, Chiba P, Ecker GF. Pharmacoinformatic approaches to design natural product type ligands of ABC-transporters. Curr. Pharm. Des. 2010; 16:1742–1752. [PubMed: 20222855]

60. Shi Z, Peng XX, Kim IW, Shukla S, Si QS, Robey RW, et al. Erlotinib (Tarceva, OSI-774) antagonizes ATP-binding cassette subfamily B member 1 and ATP-binding cassette subfamily G member 2-mediated drug resistance. Cancer Res. 2007; 67:11012–11020. [PubMed: 18006847]

61. Hegedus C, Ozvegy-Laczka C, Apati A, Magocsi M, Nemet K, Orfi L, et al. Interaction of nilotinib, dasatinib and bosutinib with ABCB1 and ABCG2: implications for altered anti-cancer effects and pharmacological properties. Br. J. Pharmacol. 2009; 158:1153–1164. [PubMed: 19785662]

62. Nakamura Y, Oka M, Soda H, Shiozawa K, Yoshikawa M, Itoh A, et al. Gefitinib ("Iressa", ZD1839), an epidermal growth factor receptor tyrosine kinase inhibitor, reverses breast cancer resistance protein/ABCG2-mediated drug resistance. Cancer Res. 2005; 65:1541–1546. [PubMed: 15735043]

63. Mi YJ, Liang YJ, Huang HB, Zhao HY, Wu CP, Wang F, et al. Apatinib (YN968D1) reverses multidrug resistance by inhibiting the efflux function of multiple ATP-binding cassette transporters. Cancer Res. 2010; 70:7981–7991. [PubMed: 20876799]
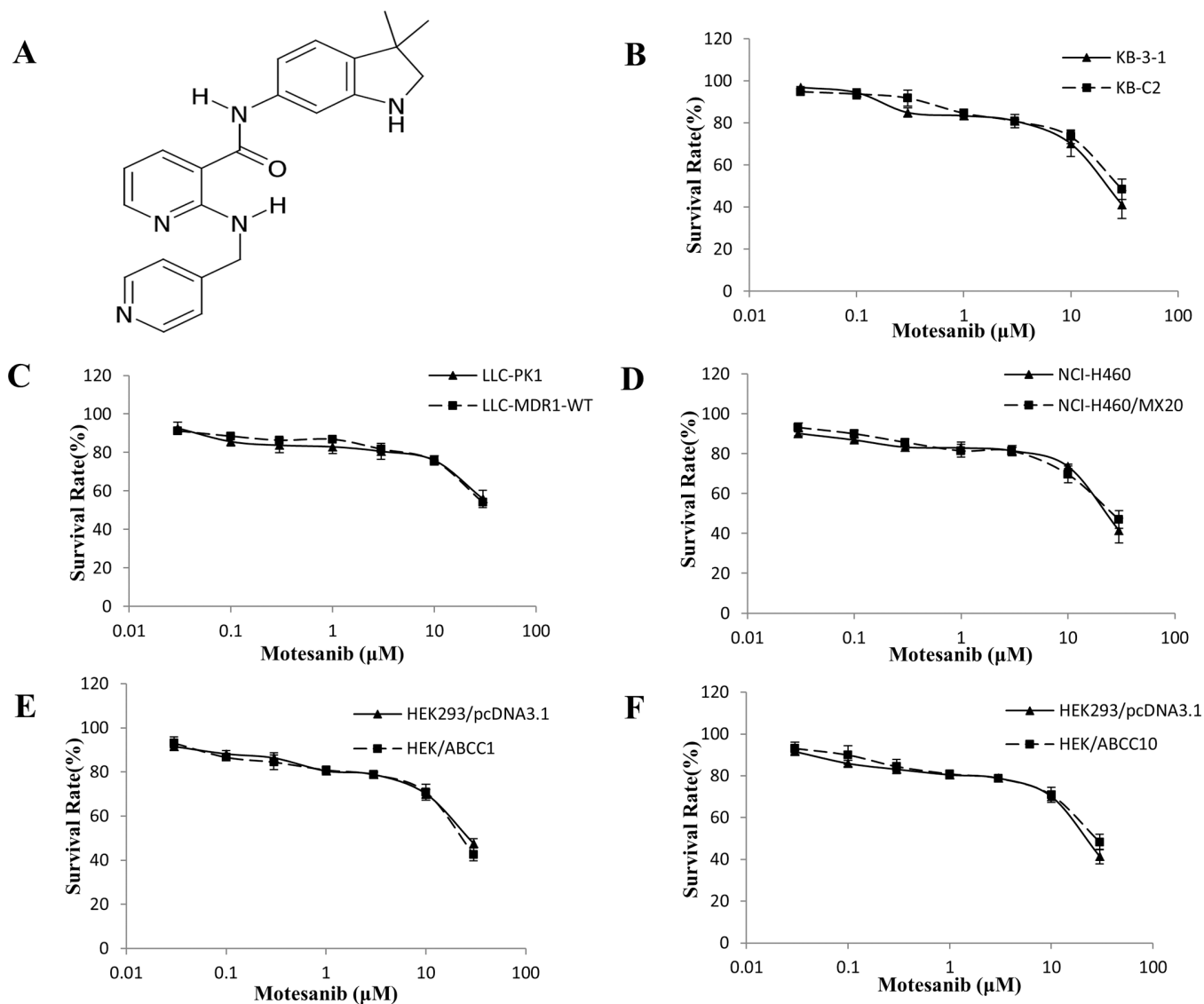
Figure 1. Chemical structure of motesanib and concentration-response curves of the cell lines treated with motesanib alone

(A) Chemical structure of motesanib (AMG706). (B) Concentration-response curves of KB-3-1 and KB-C2 cell lines treated with motesanib alone. (C) Concentration-response curves of LLC-PK1 and LLC-MDR1-WT cell lines treated with motesanib alone. (D) Concentration-response curves of NCI-H460 and NCI-H460/MX20 cell lines treated with motesanib alone. (E) Concentration-response curves of HEK293/pcDNA3.1 and HEK/ABCC1 cell lines treated with motesanib alone. (F) Concentration-response curves of HEK293/pcDNA3.1 and HEK/ABCC10 cell lines treated with motesanib alone. Each cell line was incubated with different concentrations of motesanib for 72 h. Cell survival rate was determined by the MTT assay as described in "Materials and methods". Points with error bars represent the mean ± SD. Each above figure is a representative of three independent experiments, each done in triplicate.
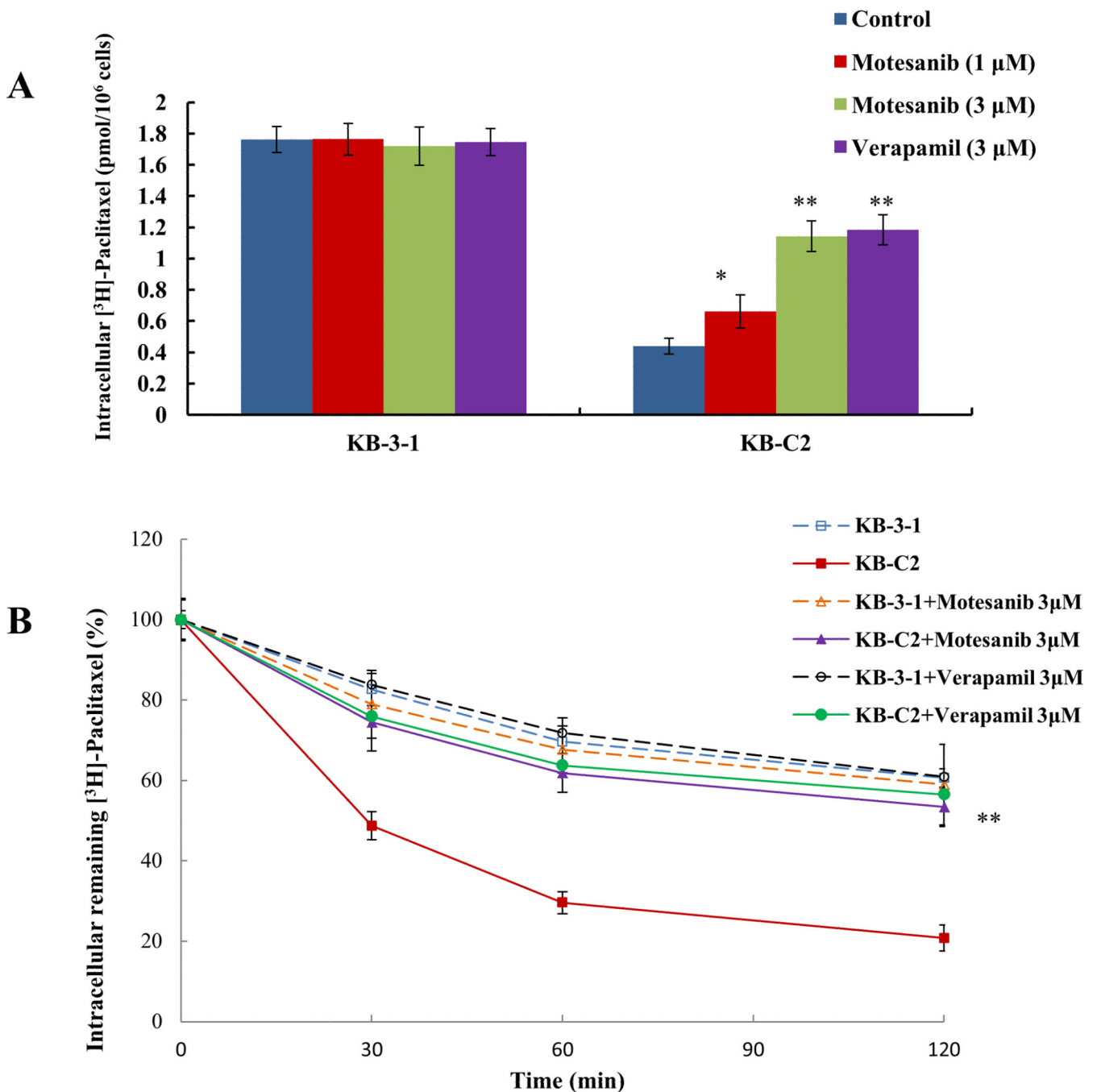
Figure 2. Effect of moteanib on the accumulation and efflux of [^{3}H]-paclitaxel
(A) The accumulation of [^{3}H]-paclitaxel was measured after the cells (parental KB-3-1 and ABCB1 overexpressing KB-C2 drug selected cell line) were pre-incubated with or without motesanib or verapamil for 2 h at 37°C and then incubated with 0.01 μM [^{3}H]-paclitaxel for another 2 h at 37°C. Columns are the mean of triplicate determinations; error bars represent SD. (B) The effect of motesanib on the efflux of [^{3}H]-paclitaxel from KB-3-1 and KB-C2 cells. Cells were pre-treated with or without motesanib or verapamil at 3 μM for 2 h at 37°C and further incubated with 0.01 μM [^{3}H]-paclitaxel at 37°C for 2 h. Cells were then

incubated in the fresh medium with or without the reversal agents for different time periods at 37°C. Cells were then collected and the intracellular levels of [^{3}H]-paclitaxel were determined by scintillation counting. A time course versus percentage of intracellular [^{3}H]-paclitaxel remaining (%) was plotted (0, 30, 60, 120 min). Lines are the mean of triplicate determinations; error bars represent SD. * indicates $P < 0.05$, ** indicates $P < 0.01$ versus the control group. The above figures are from three independent experiments, each done in triplicate.
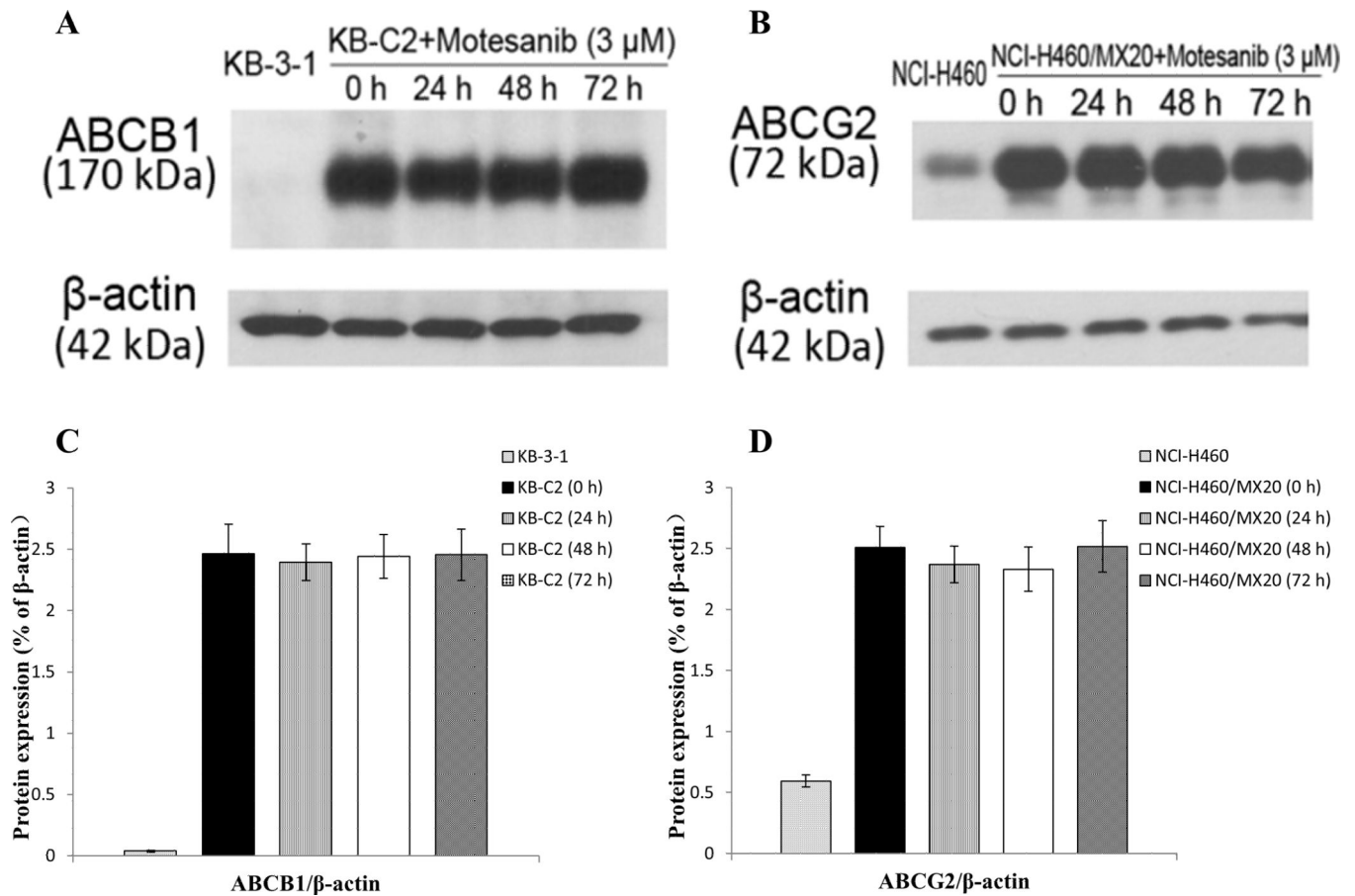
Figure 3. Western blot analysis showing the expression of ABCB1 and ABCG2 at different time points after exposure to 3 μM motesanib

Expression of ABCB1 in (A) KB-3-1 and KB-C2 and expression of ABCG2 in (B) NCI-H460 and NCI-H460/MX20. (A) Effect of motesanib at 3 μM on expression level of ABCB1 in KB-C2 cells for 0, 24, 48 and 72 h. (B) Effect of motesanib at 3 μM on expression level of ABCG2 in NCI-H460/MX20 cells for 0, 24, 48 and 72 h. The protein expression was quantified by ImageJ 1.47v Software (C, D). Equal amounts (60 μg) of cell lysates were loaded into each well and subjected to Western blot analysis as described in "Materials and methods". Representative result is shown here and similar results were obtained in two other independent trials.
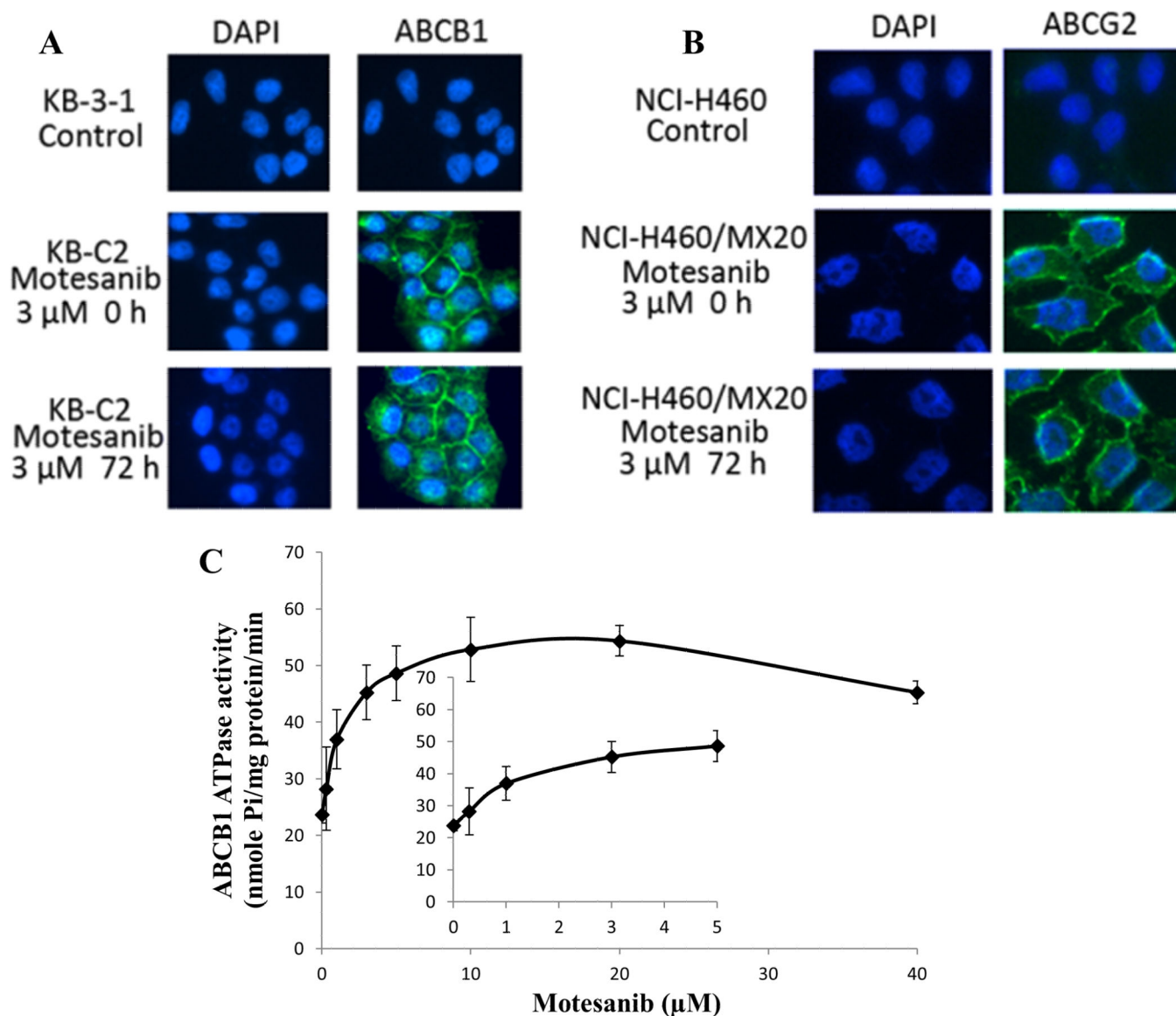
Figure 4. Effect of motesanib on the subcellular localization of ABCB1 and ABCG2, and effect of motesainib on the Vi-sensitive ABCB1 ATPase activity

(A) Effect of motesanib at 3 μM on the subcellular localization of ABCB1 in KB-C2 cells for 72 h. (B) Effect of motesanib at 3 μM on the subcellular localization of ABCG2 in NCI-H460/MX20 cells for 72 h. ABCB1 and ABCG2 staining are shown in green. DAPI (blue) counterstains the nuclei. (C) Crude membranes (100 μg protein/ml) from High-five cells expressing ABCB1 were incubated with increasing concentrations of motesanib (0–40 μM), in the presence and absence of sodium orthovanadate (Vi) (0.3 mM), in ATPase assay buffer as described in ''Materials and methods''. The inset shows stimulation of ATP hydrolysis at lower (0–5 μM) concentration of motesanib.
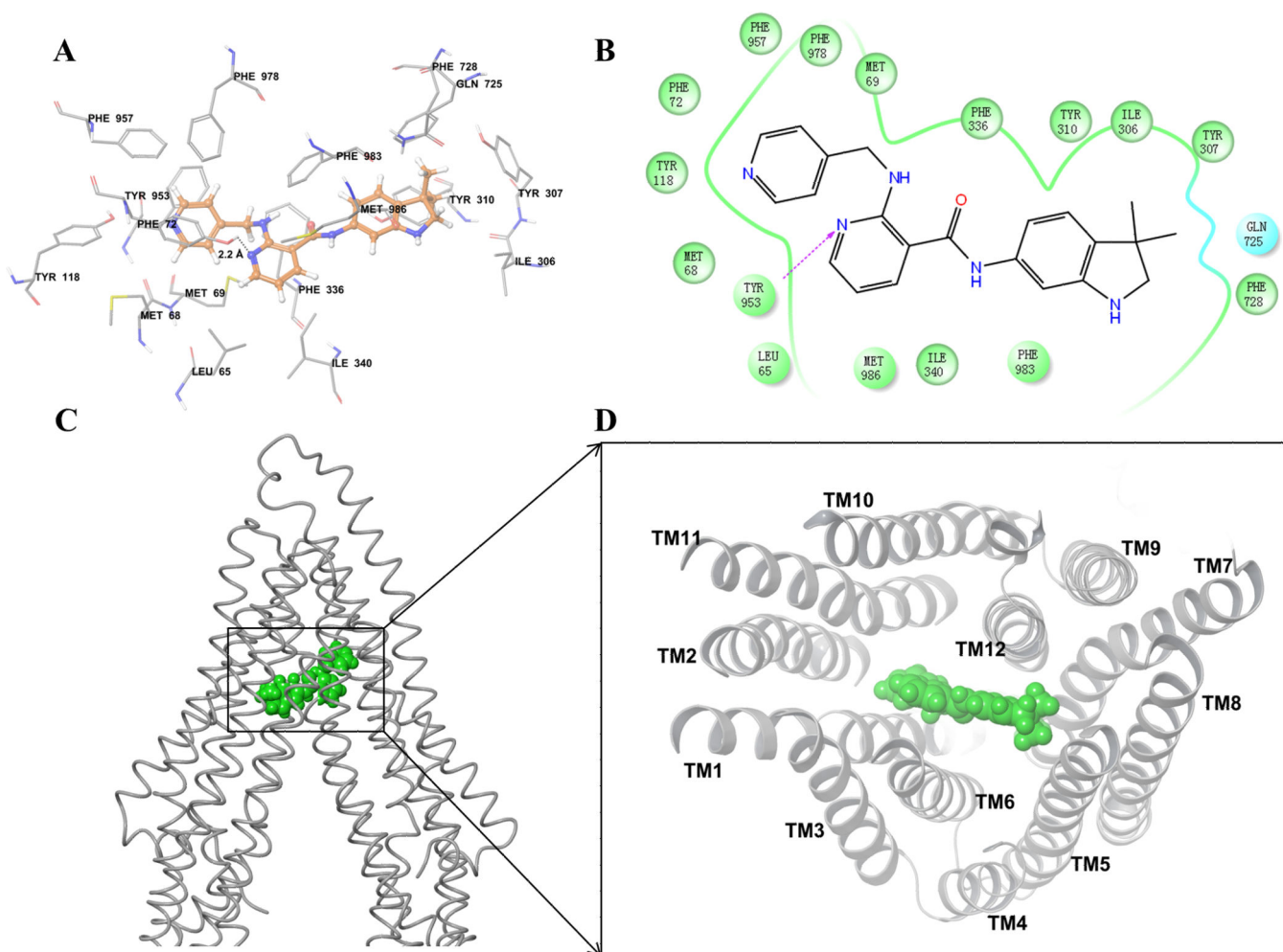
Figure 5. Docking analysis with human ABCB1 homology model
(A) XP-Glide predicted binding model of motesanib with the homology modeled human ABCB1. Important amino acids are depicted as sticks with the atoms colored as carbon – green, hydrogen – white, nitrogen –blue, oxygen – red, whereas motesanib is shown with the same color scheme as above except carbon atoms are represented in orange. Dotted black line indicates hydrogen bond. (B) A two dimensional ligand-receptor interaction diagram with important interactions observed in the docked complex of motesanib with the drug-binding site residues of human ABCB1 is shown. Residues are shown as colored bubbles, cyan indicates polar and green indicates hydrophobic residues. Hydrogen bond is shown by purple dotted arrow. (C) Binding of motesanib on ABCB1. Location of motesanib (green spheres) is shown in the ABCB1 internal large cavity. (D) Stereo images showing interactions of transmembrane helices with motesanib (green spheres) viewed from the intracellular side of the protein looking into the internal chamber.

Table 1

Motesanib reverses the ABCB1-mediated drug resistance to paclitaxel, colchicine and vincristine.

Treatment	KB-3-1		KB-C2	
	$IC_{50} \pm SD^a$ (μM)	RF^b	$IC_{50} \pm SD$(μM)	RF
Paclitaxel	0.0025 ± 0.0002	[1.0]	0.650 ± 0.039	[260.0]
+Motesanib (1 μM)	0.0026 ± 0.0001	[1.0]	$0.123 \pm 0.027^*$	[49.2]
+Motesanib (3 μM)	0.0027 ± 0.0001	[1.1]	$0.020 \pm 0.007^*$	[8.0]
+Verapamil (3 μM)	0.0025 ± 0.0002	[1.0]	$0.017 \pm 0.006^*$	[6.8]
Colchicine	0.0064 ± 0.0005	[1.0]	1.519 ± 0.043	[237.3]
+Motesanib (1 μM)	0.0061 ± 0.0006	[1.0]	$0.272 \pm 0.037^*$	[42.5]
+Motesanib (3 μM)	0.0059 ± 0.0006	[0.9]	$0.120 \pm 0.018^*$	[18.7]
+Verapamil (3 μM)	0.0058 ± 0.0008	[0.9]	$0.090 \pm 0.008^*$	[14.1]
Vincristine	0.0054 ± 0.0014	[1.0]	0.717 ± 0.019	[132.8]
+Motesanib (1 μM)	0.0054 ± 0.0008	[1.0]	$0.083 \pm 0.007^*$	[15.4]
+Motesanib (3 μM)	0.0044 ± 0.0005	[0.8]	$0.021 \pm 0.002^*$	[3.9]
+Verapamil (3 μM)	0.0033 ± 0.0013	[0.6]	$0.020 \pm 0.003^*$	[3.7]
Cisplatin	2.467 ± 0.079	[1.0]	2.363 ± 0.109	[1.0]
+Motesanib (3 μM)	2.710 ± 0.169	[1.1]	2.551 ± 0.186	[1.0]
+Verapamil (3 μM)	2.327 ± 0.070	[0.9]	2.724 ± 0.208	[1.1]

Treatment	LLC-PK1		LLC-MDR1-WT	
	$IC_{50} \pm SD^a$ (μM)	RF^b	$IC_{50} \pm SD$(μM)	RF
Paclitaxel	0.025 ± 0.002	[1.0]	1.028 ± 0.070	[41.1]
+Motesanib (1 μM)	0.025 ± 0.001	[1.0]	$0.182 \pm 0.018^*$	[7.3]
+Motesanib (3 μM)	0.023 ± 0.001	[0.9]	$0.039 \pm 0.003^*$	[1.6]
+Verapamil (3 μM)	0.024 ± 0.001	[1.0]	$0.036 \pm 0.003^*$	[1.4]
Cisplatin	1.919 ± 0.118	[1.0]	1.923 ± 0.113	[1.0]
+Motesanib (3 μM)	1.919 ± 0.116	[1.0]	1.924 ± 0.125	[1.0]
+Verapamil (3 μM)	1.854 ± 0.125	[1.0]	1.835 ± 0.078	[1.0]

a IC_{50} values are represented as mean ± SD of at least three independent experiments performed in triplicate.

b Values represent the resistance fold (RF) obtained by dividing IC_{50} value of antineoplastic drugs in KB-3-1 and KB-C2 cells with or without reversal agent divided by the IC_{50} value of respective antineoplastic drug in KB-3-1 cells without reversal agent. The RF for LLC-PK1 and LLC-MDR1-WT cells was obtained in the similar manner. Cell survival assay was determined by the MTT assay as described in Section 2. Verapamil was used as a positive control of ABCB1 inhibitor.

$*$ $P < 0.01$ versus the control group without reversal agent.

Table 2

Motesanib reverses the ABCG2-mediated drug resistance to mitoxantrone.

Treatment	NCI-H460		NCI-H460/MX20	
	$IC_{50} \pm SD^a$ (µM)	FR^b	$IC_{50} \pm SD$(µM)	FR
Mitoxantrone	0.012 ± 0.001	[1.0]	1.625 ± 0.102	[135.4]
+Motesanib (3 µM)	0.010 ± 0.001	[0.8]	$0.564 \pm 0.012^*$	[47.0]
+FTC (3 µM)	0.007 ± 0.001	[0.6]	$0.049 \pm 0.004^*$	[4.1]
Cisplatin	1.403 ± 0.028	[1.0]	1.347 ± 0.007	[1.0]
+Motesanib (3 µM)	1.383 ± 0.026	[1.0]	1.353 ± 0.051	[1.0]
+FTC (3 µM)	1.360 ± 0.082	[1.0]	1.327 ± 0.055	[0.9]

[a] IC_{50} values are represented as mean ± SD of at least three independent experiments performed in triplicate.

[b] Values represent the resistance fold (RF) obtained by dividing IC_{50} value of antineoplastic drugs in NCI-H460 and NCI-H460/MX20 cells with or without reversal agent divided by the IC_{50} value of respective antineoplastic drug in NCI-H460 cells without reversal agent. Cell survival assay was determined by the MTT assay as described in Section 2. FTC was used as a positive control of ABCG2 inhibitor.

[*] $P < 0.01$ versus the control group without reversal agent.

Table 3

Motesanib does not show any effect on the ABCC1-and ABCC10-mediated multidrug resistance.

Treatment	HEK293/pcDNA3.1		HEK/ABCC1	
	$IC_{50} \pm SD^a$ (μM)	FR^b	$IC_{50} \pm SD$ (μM)	FR
Vincristine	0.021 ± 0.002	[1.0]	0.582 ± 0.027	[27.7]
+#28 (1.5 μM)	0.021 ± 0.002	[1.0]	0.569 ± 0.019	[27.1]
+PAK-104P (2.5 μM)	0.020 ± 0.002	[1.0]	0.112 ± 0.008[*]	[5.3]

Treatment	HEK293/pcDNA3.1		HEK/ABCC10	
	$IC_{50} \pm SD^a$ (μM)	FR^b	$IC_{50} \pm SD$ (μM)	FR
Paclitaxel	0.0082 ± 0.0007	[1.0]	0.0754 ± 0.0052	[9.2]
+Motesanib (1.5 μM)	0.0077 ± 0.0008	[0.9]	0.0719 ± 0.0051	[8.8]
+Cepharanthine (2.5 μM)	0.0066 ± 0.0007	[0.8]	0.0091 ± 0.0006[*]	[1.1]

[a]IC_{50} values are represented as mean ± SD of at least three independent experiments performed in triplicate.

[b]Values represent the resistance fold (RF) obtained by dividing IC_{50} value of antineoplastic drugs in HEK293/pcDNA3.1, HEK/ABCC1 and HEK/ABCC10 cells with or without reversal agent divided by the IC_{50} value of respective antineoplastic drug in HEK293/pcDNA3.1 cells without reversal agent. Cell survival assay was determined by the MTT assay as described in Section 2. PAK-104P was used as a positive control of ABCC1 inhibitor. Cepharanthine was used as a positive control of ABCC10 inhibitor.

[*]$P < 0.01$ versus the control group without reversal agent.